Contents

List of Abbreviations

List of Symbols

$\mathcal{F}$	Free Energy
$\mathcal{U}$	Internal Energy
$\mathcal{Z}$	Partition Function
$\mathcal{S}$	Entropy
m	Mass
p	Pressure
ρ	Density

Units

This thesis uses the geometrized unit system $G = c = 1$. If not otherwise mentioned any variable named G or c can be set to 1 and is only written for clarification.

List of Figures

List of Tables

1 Introduction

The theory of General Relativity (GR) has allowed scientists deep insights into space and time itself. Of the plentiful present problems one in particular of significant importance has been to describe the macroscopic properties of spherically symmetric stellar objects. Stars, black holes, galaxies and clusters are just a few examples of this category.

2 Thermodynamic Calculation of an EoS

This chapter aims at developing an fully special relativistic Equation of State (EoS) of a noninteracting gas. We briefly summarise important concepts necessary for the derivation. In the canonical ensemble, for which a introduction can be found in [Fli18], the internal energy $\mathcal{U}$ is obtained by the relation $\mathcal{U} = \mathcal{F} - TS$ where the quantities $\mathcal{F}$ and S can be derived by means of the partition function $\mathcal{Z}$ while T is a variable. Microscopically the partition function is given by the behaviour of the N particles determined by the Hamiltonian H. Concepts and definitions of Hamilton Mechanics can be found in [Esc11; Fli20; Spiec]. In general we assume $H : \mathbb{R}^{3N} \times \mathbb{R}^{3N} \to \mathbb{R}$ to be a positive smooth function that assigns the positions and momenta of N particles an energy. This explicitly takes form in the well known equations

$$\mathcal{Z}(T,V,N) = \int\limits_{\mathcal{V}\times\mathbb{R}^N} \exp\left(-\frac{H(x_1,\dots,x_N,p_1,\dots,p_N)}{k_B T}\right) \frac{\mathrm{d}x_1\,\mathrm{d}p_1\dots\mathrm{d}x_N\,\mathrm{d}p_N}{N!h^{3N}} \tag{2.0.1}$$

$$\mathcal{F}(T,V,N) = -k_B T \log\left(\mathcal{Z}(T,V,N)\right) \tag{2.0.2}$$

$$\mathcal{U}(T,V,N) = \mathcal{F} + T\mathcal{S} \;=\; \mathcal{F} - T\frac{\partial \mathcal{F}}{\partial T} \;=\; k_B T^2 \frac{1}{\mathcal{Z}}\frac{\partial \mathcal{Z}}{\partial T} \tag{2.0.3}$$

where $x_i \in \mathcal{V} \subset \mathbb{R}^N$ and $p_i \in \mathbb{R}^N$. The relation $V = \mathrm{vol}(\mathcal{V})$ describes the total volume occupied by the medium while T and N are its temperature and particle number respectively. To fully calculate U it is necessary to obtain the partition function $\mathcal{Z}$. From there $\mathcal{U}/V$ as the energy density can be compared to the pressure defined by

$$p = \frac{\mathrm{d}\mathcal{F}}{\mathrm{d}V}. \tag{2.0.4}$$

to yield an EoS.

2.1 The Ultra-Relativistic Internal Energy

The ultra-relativistic case is a textbook example and well known limit that we will use in order to verify our later calculated results. First we write down the ultra-relativistic Hamiltonian given by

$$H(x,p) = ||p||c. \tag{2.1.1}$$

The corresponding partition function for a N particle system then reads ($\beta = (k_B T)^{-1}$)

$$\mathcal{Z} = \frac{V^N}{N!h^{3N}} \left[\int\limits_{\mathbb{R}^3} \exp\left(-\beta H(p)\right) \mathrm{d}^3 p\right]^N \tag{2.1.2}$$

$$= \frac{V^N}{N!h^{3N}} \left[\int\limits_0^\infty 4\pi p^2 \exp(-\beta p c)\,\mathrm{d}p\right]^N \tag{2.1.3}$$

$$= \frac{V^N}{N!h^{3N}} \frac{(4\pi)^N}{(\beta c)^{3N}} \left[\int\limits_0^\infty x^2 \exp(-x)\,\mathrm{d}x\right]^N \tag{2.1.4}$$

$$\mathcal{Z} = \frac{1}{N!}\left(8\pi V \left(\frac{k_B T}{hc}\right)^3\right)^N \tag{2.1.5}$$

where from the first to second line we used usual spherical coordinates and afterwards the integral transformation $x = \beta cp$. The integral in equation (2.1.4) can be solved exactly with value 2. In the last line $\beta = (k_B T)^{-1}$ was used for visual clarity. With equation (2.0.3) the internal energy $\mathcal{U} = 3Nk_BT$ and with equation (2.0.4) the EoS can now be written down

$$p = \frac{Nk_BT}{V} = \frac{1}{3}\frac{\mathcal{U}}{V} = \frac{1}{3}\rho. \tag{2.1.6}$$

2.2 The Special-Relativistic Internal Energy

A source for the following calculations could not be found and were thus carried out by the author solely. The special relativistic Hamiltonian is given by

$$H = mc^2\sqrt{1 + \frac{p^2}{m^2c^2}}. \tag{2.2.1}$$

The ultra-relativistic limit can be obtained by letting $m \to 0$. In this limiting case we should be able to recover the results from equation (2.1.5).

$$\mathcal{Z} = \frac{V^N}{N!h^{3N}}\left[\int_{\mathbb{R}^3} \exp\left(-\frac{mc^2\sqrt{1+\frac{p^2}{m^2c^2}}}{k_BT}\right) \mathrm{d}^3p\right]^N \tag{2.2.2}$$

$$= \frac{V^N}{N!h^{3N}}\left[\int_0^\infty 4\pi p^2 \exp\left(-\beta mc^2\sqrt{1+\frac{p^2}{m^2c^2}}\right) \mathrm{d}p\right]^N \tag{2.2.3}$$

$$= \frac{(4\pi V)^N}{N!}\left(\frac{mc}{h}\right)^{3N}\left[\int_0^\infty q^2 \exp\left(-\alpha\sqrt{1+q^2}\right) \mathrm{d}q\right]^N \tag{2.2.4}$$

$$= \frac{(4\pi V)^N}{N!}\left(\frac{mc}{h}\right)^{3N}\left(\int_0^\infty \sinh(x)^2\cosh(x)\exp(-\alpha\cosh(x))\,\mathrm{d}x\right)^N \tag{2.2.5}$$

$$= \frac{(4\pi V)^N}{N!}\left(\frac{mc}{h}\right)^{3N}\left(\int_0^\infty \frac{\sinh(2x)}{2}\sinh(x)\exp(-\alpha\cosh(x))\,\mathrm{d}x\right)^N \tag{2.2.6}$$

$$= \frac{(4\pi V)^N}{N!}\left(\frac{mc}{h}\right)^{3N}\left(-\frac{\sinh(2x)}{2\alpha}\exp(-\alpha\cosh(x))\Big|_0^\infty\right. \tag{2.2.7}$$

$$\left. + \frac{1}{\alpha}\int_0^\infty \cosh(2x)\exp(-\alpha\cosh(x))\,\mathrm{d}x\right)^N \tag{2.2.8}$$

$$= \frac{(4\pi V)^N}{N!}\left(\frac{mc}{h}\right)^{3N}\left(\frac{1}{\alpha}\int_0^\infty \cosh(2x)\exp(-\alpha\cosh(x))\,\mathrm{d}x\right)^N \tag{2.2.9}$$

$$= \frac{1}{N!}\left(8\pi V\left(\frac{k_BT}{hc}\right)^3\frac{\alpha^2K_2(\alpha)}{2}\right)^N \tag{2.2.10}$$

In the first step we used spherical coordinates followed by the substitution $qmc = p$ and $\alpha = \beta mc^2 = mc^2/k_BT$. Afterwards we substituted $q = \sinh(x)$ and used the identity $\cosh(x)\sinh(x) = \sinh(2x)/2$. Partial integration then leads to the last integral which can be identified as the modified Bessel function of the 2nd kind $K_2(\alpha)$ [AS84]. The equation is then rewritten such that the ultra-relativistic limit can be read off upon letting $\alpha \to 0$. We can now calculate the internal energy $\mathcal{U}$ from $\mathcal{Z}$ via equation (2.0.3)

$$\mathcal{U} = 3Nk_BT - Nk_BT\alpha\left(\frac{\partial_\alpha K_2(\alpha)}{K_2(\alpha)} + 2\right) \tag{2.2.11}$$

$$\mathcal{U} = 3Nk_BT - mc^2\left(\frac{\partial_\alpha K_2(\alpha)}{K_2(\alpha)} + 2\right). \tag{2.2.12}$$

Again, it can be seen that the ultra-relativistic limit can be obtained by letting $\alpha \to 0$ since the term written in brackets vanishes. It is immediate that the ultra-relativistic EoS is $\rho = 3p$ which is equivalent to a traceless energy momentum tensor.
From equation (2.2.10) and (2.0.2), we immediately derive the ideal gas equation via the definition of pressure (see equation (2.0.4) in the canonical ensemble

$$p = \frac{\partial \mathcal{F}}{\partial V} = \frac{Nk_BT}{V}. \tag{2.2.13}$$

Note that in the case of the Hamiltonian H having a non-trivial dependence on the coordinates x_i, the partition function would differ by a factor involving V and T. This more general scenario does not yield the ideal gas law and would thus need to be treated separately.

2.3 The Special-Relativistic Equation of State

This section aims to develop an equation between the thermodynamic energy density $\rho = \mathcal{U}/V$ and the pressure p of the gas given by the ideal gas equation (2.0.4). We assume an additional constraint namely adiabaticity and thus further reduce the degrees of freedom of the thermodynamic system.
When assuming an adiabatic condition $\delta Q = 0$ and using the First Law of Thermodynamics [Fli18] $\mathrm{d}U = \delta Q + \delta W$, where $\delta W = -p\,\mathrm{d}V$ and $\mathrm{d}U = C_V\,\mathrm{d}T$, we can relate pressure and temperature. This adiabatic condition is quite well satisfied since the time scale of radiational and other losses compared to the time scale of thermodynamic events is negligible [Noe08; Vin17]. Using equation (2.2.12) and (2.0.4), we obtain

$$-p\,\mathrm{d}V = C_V\,\mathrm{d}T \tag{2.3.1}$$

$$-\frac{Nk_BT}{V}\,\mathrm{d}V = Nk_B\left[1+\alpha^2\left(\left(\frac{\partial_\alpha K_2(\alpha)}{K_2(\alpha)}\right)^2 - \frac{\partial_\alpha^2 K_2(\alpha)}{K_2(\alpha)}\right)\right]\mathrm{d}T \tag{2.3.2}$$

$$-\frac{\mathrm{d}V}{V} = \left[1-\alpha^2\partial_\alpha\left(\frac{\partial_\alpha K_2(\alpha)}{K_2(\alpha)}\right)\right]\frac{\mathrm{d}T}{T} \tag{2.3.3}$$

$$= \left[1-\alpha^2\partial_\alpha^2\left(\log K_2(\alpha)\right)\right]\frac{\mathrm{d}T}{T} \tag{2.3.4}$$

This equation also shows explicitly the T dependence of the specific heat C_V for the general case. Again, taking the ultra-relativistic limit by taking $\alpha \to 0$, one can calculate

that the right hand term in the first equation converges to $-2Nk_B$. This agrees with the expected specific heat for an ultra-relativistic gas $C_{V,\mathrm{ur}} = 3Nk_B$. With the identity $\mathrm{d}\alpha/\alpha = -\,\mathrm{d}T/T$ (using $\alpha = mc^2/k_BT$), we can transform the equation and integrate it. After applying partial integration, the result is

$$\frac{\mathrm{d}V}{V} = \left(1 - \alpha^2\partial_\alpha^2 \log K_2(\alpha)\right)\frac{\mathrm{d}\alpha}{\alpha} \tag{2.3.5}$$

$$\log\left(\frac{V}{V_0}\right) = \log\left(\frac{\alpha}{\alpha_0}\right) - \int_{\alpha_0}^{\alpha} \alpha\frac{\partial^2}{\partial\alpha^2}\log(K_2(\alpha'))\,\mathrm{d}\alpha' \tag{2.3.6}$$

$$= \log\left(\frac{\alpha}{\alpha_0}\right) + \log\left(\frac{K_2(\alpha)}{K_2(\alpha_0)}\right) - \left[\alpha\frac{\partial_\alpha K_2}{K_2}\right]_{\alpha_0}^{\alpha} \tag{2.3.7}$$

This equation enables us to write down a relation between volume and temperature (encapsulated in $\alpha = mc^2/k_BT$)

$$V(\alpha) = \frac{\alpha K_2(\alpha)}{C}\exp\left(\alpha\frac{K_3(\alpha) + K_1(\alpha)}{2K_2(\alpha)}\right) \tag{2.3.8}$$

where the constant C is defined by the equation beforehand and only depends on the integration boundaries α_0 and V_0. It is given by

$$C = \frac{\alpha_0 K_2(\alpha_0)}{V_0}\exp\left(\alpha_0\frac{K_1(\alpha_0) + K_3(\alpha_0)}{2K_2(\alpha_0)}\right). \tag{2.3.9}$$

Since the goal of this section is to obtain a readable output for an EoS, it is necessary to construct a bijection relating p and T. This is made clear when writing down the energy density

$$\rho = \frac{\mathcal{U}}{V} = \frac{Nk_BT}{V} - \frac{Nk_BT}{V}\left(\alpha\frac{\partial_\alpha K_2(\alpha)}{K_2(\alpha)}\right) \tag{2.3.10}$$

where $p = Nk_BT/V$ can be easily identified but the T dependence via α is not solved yet. The pressure p can be rewritten to take the form

$$p = \frac{Nk_BT}{V} = CNmc^2\frac{1}{K_2(\alpha)\alpha^2}\exp\left(-\alpha\frac{K_1(\alpha) + K_3(\alpha)}{2K_2(\alpha)}\right). \tag{2.3.11}$$

At this point it is not reasonable to ask what happens in the ultra-relativistic limit since C depends non-trivially on m and m thus is not fully substituted in α.
Interestingly, the pressure seems to be constant for very high temperatures. The limiting case is obtained when taking $T \to \infty$ (which corresponds to $\alpha \to 0$)

$$\lim_{\alpha\to 0}\left[\frac{1}{K_2(\alpha)\alpha^2}\exp\left(-\alpha\frac{K_1(\alpha) + K_3(\alpha)}{2K_2(\alpha)}\right)\right] = \frac{1}{2e^2} \approx 0.006767. \tag{2.3.12}$$

The same argument then holds true for the density given by equation (2.3.10) and since

$$\lim_{\alpha\to 0}\left[1 + \alpha\frac{K_1(\alpha) + K_3(\alpha)}{2K_2(\alpha)}\right] = 3 \tag{2.3.13}$$

we have

$$\lim_{\alpha\to 0}\left(\frac{\rho(\alpha)}{Cmc^2}\right) = \frac{3}{2e^2} \approx 0.203003. \tag{2.3.14}$$

Theorem 2.1
The mapping $p : \mathbb{R}_{>0} \to \mathbb{R}_{>0}, \alpha \mapsto p(\alpha)$ written down in equation (2.3.11) is a bijection for any $N, m, c, C \neq 0$.

$$p = \frac{Nk_BT}{V} = CNmc^2 \frac{1}{K_2(\alpha)\alpha^2} \exp\left(-\alpha \frac{K_1(\alpha) + K_3(\alpha)}{2K_2(\alpha)}\right) \tag{2.3.15}$$

Proof. For this proof it suffices to show that the function $p(\alpha)$ has a strictly monotonous behaviour. Without loss of generality, we assume $N, m, c, C > 0$. Now it is obvious that the first two terms $Nmc^2/CK_2(\alpha)$ and α^{-2} are strictly decreasing. This is easy to see when using [AS84]

$$\frac{\partial K_n}{\partial \alpha} = \frac{n}{\alpha} K_n - K_{n+1} = -\frac{K_{n-1} + K_{n+1}}{2}. \tag{2.3.16}$$

We then calculate the derivative of the third term and divide by the exponential (since it is positive)

$$\frac{1}{\exp(\alpha \partial_\alpha \log(K_2))} \frac{\partial}{\partial \alpha} \exp(\alpha \partial_\alpha \log(K_2)) \tag{2.3.17}$$

$$= \partial_\alpha \log(K_2) + \alpha \partial_\alpha^2 \log(K_2) \tag{2.3.18}$$

$$= \frac{\partial_\alpha K_2}{K_2} + \alpha \frac{\partial_\alpha^2 K_2}{K_2} + \alpha \left(\frac{\partial_\alpha K_2}{K_2}\right)^2 \tag{2.3.19}$$

$$= \frac{K_1 - \frac{2}{\alpha} K_2}{K_2} + \alpha \frac{\frac{1}{\alpha} K_1 - K_2 - \frac{2}{\alpha}\left(K_1 - \frac{2}{\alpha} K_2\right) + \frac{2}{\alpha^2} K_2}{K_2^2} + \alpha \frac{K_1^2 - \frac{1}{\alpha} K_1 K_2 - \frac{4}{\alpha^2} K_2^2}{K_2^2} \tag{2.3.20}$$

$$= -\alpha + \alpha \frac{K_1^2}{K_2^2} - 4 \frac{K_1}{K_2} \tag{2.3.21}$$

thus it is sufficient to show that

$$\alpha \frac{K_1^2}{K_2^2} < \alpha + 4 \frac{K_1}{K_2}. \tag{2.3.22}$$

We quickly prove the more general result $K_\nu < K_{\nu+1}$. One possible definition [AS84] for the Bessel function K_ν is given by

$$K_\nu := \frac{\sqrt{\pi}}{(\nu - \frac{1}{2})!} \left(\frac{1}{2} z\right)^\nu \int_1^\infty e^{-tz} \left(t^2 - 1\right)^{\nu - \frac{1}{2}} \mathrm{d}t \tag{2.3.23}$$

We inspect the ratio

$$\frac{K_\nu}{K_{\nu+1}} = \frac{1}{\left(\nu + \frac{1}{2}\right)\left(\frac{1}{2} z\right)} \frac{\int e^{-tz} \left(t^2 - 1\right)^{\nu - 1/2} \mathrm{d}t}{\int e^{-tz} \left(t^2 - 1\right)^{\nu + 1/2} \mathrm{d}t} \tag{2.3.24}$$

and rewrite the demoninator with partial integration

$$\frac{1}{2} z \int_1^\infty e^{-tz} \left(t^2 - 1\right)^{\nu + 1/2} \mathrm{d}t = \left(\nu + \frac{1}{2}\right) \int_1^\infty e^{-tz} t \left(t^2 - 1\right)^{\nu - 1/2} \mathrm{d}t. \tag{2.3.25}$$

Now it is obvious that $K_{\nu+1} > K_\nu$. Thus in total, the function given by equation (2.3.26) can be inverted. □

With this mapping $p : \mathbb{R}_{>0} \to \mathbb{R}_{>0}, \alpha \mapsto p(\alpha)$ and its inverse $\alpha : \mathbb{R}_{>0} \to \mathbb{R}_{>0}, p \mapsto \alpha(p)$, we can use (2.3.10) and finally write down the EoS

$$\rho = \frac{\mathcal{U}}{V} = p\left(1 + \alpha(p)\frac{K_1(\alpha(p)) + K_3(\alpha(p))}{2K_2(\alpha(p))}\right). \tag{2.3.26}$$

Figure 1 is obtained by choosing numerical values and then interpolating and inverting equation (2.3.11). The constant factor

$$B := CNmc^2/p_0 \tag{2.3.27}$$

is substituted to obtain independence of p_0[1]. Furthermore the graphs of the plotted EoS are normalised such that

$$\rho_i(p_0) = \rho_{0,i} \tag{2.3.28}$$

and can thus be compared with each other. Note that the ρ_0 of the plot is not a universal value but rather each function has been scaled individually and ρ_0 is a placeholder for the corresponding $\rho_{0,i}$. The polytropic EoS $\rho_{cla}(p) = Ap^{1/\gamma}$ when normalised as before the equation is independent of A and can be uniquely characterised by n. For further details, the interested reader is referred to [Ple21].

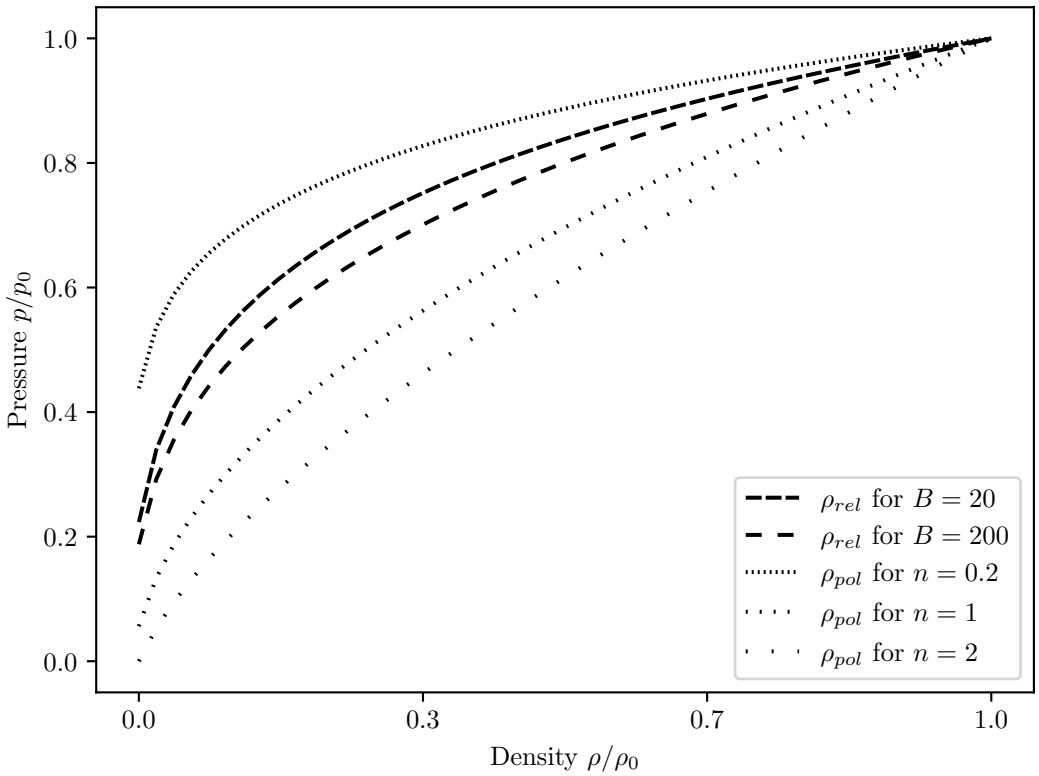

Figure 1: Relativistic Equation of State - The relativistic EoS $\rho(p)$ is normalised such that values can be compared with a polytropic EoS. Graphs for the relativistic version are independent of the exponent n which is a degree of freedom intrinsic to the polytropic EoS. By normalisation, the graphs of the polytropic EoS are independent of the factor A.

[1]This will be the starting value for the pressure in the Tollmann-Oppenheimer-Vollkoff equation. Since the pressure decreases from the inside of a star to the outside, this resembles our highest value of p.

3 Calculating the Mass of a Star with an EOS

3.1 Deriving the TOV-Equation

Information about GR can be found in [CD00; Cho09; Cho15; Wal84]. We follow the derivation of Wald. In this chapter, we consider a spherical-symmetric static Lorentz-Manifold (V, g) with charts such that the metric g can be written as

$$g = -e^{\nu}dt^2 + e^{\lambda}dr^2 + r^2(d\theta^2 + \sin^2\theta d\phi^2). \tag{3.1.1}$$

The stress-energy tensor of an ideal fluid with density ρ and pressure p is given by

$$T_{\mu\nu} = \rho u_\mu u_\nu + p(g_{\mu\nu} + u_\mu u_\nu) \tag{3.1.2}$$

where u is the 4-velocity of the fluid. In the rest frame where $u^\mu = (-e^{-\nu/2}, 0, 0, 0)$, this equation simplifies to

$$T^\mu_\nu = \mathrm{diag}(-\rho, p, p, p) \tag{3.1.3}$$

The Christoffel symbols for this metric are

$$\Gamma^0_{\mu\nu} = \begin{bmatrix} 0 & \nu'/2 & & \\ \nu'/2 & 0 & & \\ & & 0 & \\ & & & 0 \end{bmatrix}, \quad \Gamma^1_{\mu\nu} = \begin{bmatrix} \nu' e^{\nu-\lambda}/2 & & & \\ & \lambda'/2 & & \\ & & -r e^{-\lambda} & \\ & & & -r\sin^2\theta e^{-\lambda} \end{bmatrix} \tag{3.1.4}$$

$$\Gamma^2_{\mu\nu} = \begin{bmatrix} 0 & & & \\ & 0 & 1/r & \\ & 1/r & 0 & \\ & & & -\sin\theta\cos\theta \end{bmatrix}, \quad \Gamma^3_{\mu\nu} = \begin{bmatrix} 0 & & & \\ & 0 & & \\ & 0 & 0 & 1/r \\ & 0 & 0 & \cos\theta/\sin\theta \\ & 1/r & \cos\theta/\sin\theta & 0 \end{bmatrix} \tag{3.1.5}$$

From these, the non-zero components of the Ricci-Tensor can be calculated

$$R_{11} = \frac{1}{4r}e^{-\lambda}\left[\left(2r\nu'' + r\nu'^2\right) + \left(4 - r\lambda'\right)\nu'\right] \tag{3.1.6}$$

$$R_{22} = -\frac{1}{4r}e^{-\lambda}\left[(2r\nu'') + r\nu'^2 - r\lambda'\nu' - 4\lambda'\right] \tag{3.1.7}$$

$$R_{33} = -\frac{1}{2r^2}e^{-\lambda}\left(r\nu' - r\lambda' - 2e^{\lambda} + 2\right) \tag{3.1.8}$$

$$R_{44} = R_{33} \tag{3.1.9}$$

and with $R_{\mu\nu} - g_{\mu\nu}R/2 = G_{\mu\nu} = 8\pi T_{\mu\nu}$ ultimately yield the following field equations.

$$-8\pi T^0_0 = 8\pi\rho = \frac{\lambda' e^{-\lambda}}{r} + \frac{1 - e^{-\lambda}}{r^2} \tag{3.1.10}$$

$$8\pi T^1_1 = 8\pi p = \nu'\frac{e^{-\lambda}}{r} - \frac{1 - e^{-\lambda}}{r^2} \tag{3.1.11}$$

$$8\pi T^2_2 = 8\pi p = \frac{e^{-\lambda}}{2}\left[\nu'' + \left(\frac{\nu'}{2} + \frac{1}{r}\right)(\nu' - \lambda')\right] \tag{3.1.12}$$

Since $R^4_4 = R^3_3$, we omitted the last equation. From equation (3.1.10) we infer the relation.

$$e^{-\lambda} = 1 - \frac{2}{r}\int_0^r 4\pi\rho(r')r'^2 dr' = 1 - \frac{2m(r)}{r}. \tag{3.1.13}$$

The metric needs to be defined at every point in space and thus we can not have any additional integration constant in equation (3.1.13), since otherwise we would obtain a term a/r which is ill defined for $r \to 0$.
The property $m(r)$ can be recognised as the Newtonian mass of the star (which is different to the proper mass [Wal84]). Since $e^{-\lambda} > 0$, we immediately see that $m(r) < r/2$.
In addition to the Field equations (3.1.10) to (3.1.12) the divergence of the Stress-Energy Tensor yields more information

$$\nabla_\mu T^{\mu\nu} = 0. \tag{3.1.14}$$

The following explicit calculation[2] shows how to obtain this additional restriction on the pressure and density.

$$\nabla_\mu T^\mu_\nu = \partial_\mu T^\mu_1 + \Gamma^\mu_{\mu\sigma} T^\sigma_\nu - \Gamma^\sigma_{\mu\nu} T^\mu_\sigma \tag{3.1.15}$$

$$\nabla_\mu T^\mu_1 = \frac{\partial p}{\partial r} + p\left(\Gamma^0_{01} + \Gamma^1_{11} + \Gamma^2_{21} + \Gamma^3_{31}\right) - \Gamma^\sigma_{\mu 1} T^\mu_\sigma \tag{3.1.16}$$

$$= \frac{\partial p}{\partial r} + p\left(\frac{\nu' + \lambda'}{2} + \frac{2}{r}\right) + \rho\frac{\nu'}{2} - p\frac{\lambda'}{2} - p\frac{2}{r} \tag{3.1.17}$$

$$\frac{\partial p}{\partial r} = -\frac{p+\rho}{2}\nu' \tag{3.1.18}$$

Together with equation (3.1.11) and the definition (3.1.13), we can write

$$\frac{\partial p}{\partial r} = -\frac{p+\rho}{2}\left(\frac{8\pi p r + \frac{1-e^{-\lambda}}{r}}{e^{-\lambda}}\right) \tag{3.1.19}$$

$$= -\frac{p+\rho}{2r}\left(\frac{8\pi p r + \frac{2m}{r^2}}{1 - \frac{2m}{r}}\right) \tag{3.1.20}$$

$$= -\frac{m\rho}{r^2}\left(1 + \frac{p}{\rho}\right)\left(\frac{4\pi r^3 p}{m} + 1\right)\left(1 - \frac{2m}{r}\right)^{-1} \tag{3.1.21}$$

$$\frac{\partial p}{\partial r} = -\frac{Gm\rho}{r^2}\left(1 + \frac{p}{\rho c^2}\right)\left(\frac{4\pi r^3 p}{mc^2} + 1\right)\left(1 - \frac{2Gm}{rc^2}\right)^{-1} \tag{3.1.22}$$

where in the last step the constants $c = G = 1$ were put back in. Equation (3.1.22) together with (3.1.13) yields the Tollmann-Oppenheimer-Vollkoff (TOV) differential equations

$$\frac{\partial m}{\partial r} = \quad 4\pi\rho(r) r^2 \tag{3.1.23}$$

$$\frac{\partial p}{\partial r} = -\frac{Gm\rho}{r^2}\left(1 + \frac{p}{\rho c^2}\right)\left(\frac{4\pi r^3 p}{mc^2} + 1\right)\left(1 - \frac{2Gm}{rc^2}\right)^{-1} \tag{3.1.24}$$

[2] Again assuming spherical symmetry.

3.2 Newtonian Limit

This section follows [Wei20] and [Cha58, pp. 89 sqq.]. Together with a polytropic EoS $p = K\rho^{1+1/n}$ and the definition $\rho = \lambda\theta^n$, we expect to obtain the Newtonian behavior in the non-relativistic limit in the form of the Lane-Emden (LE) equation

$$\frac{K(n+1)\lambda^{1/n-1}}{4\pi}\Delta\theta + \theta^n = 0. \tag{3.2.1}$$

The usual non-relativistic limit is obtained from a Taylor expansion of equation (3.1.24) around $1/c^2$ in lowest order. The resulting equation then reads

$$\frac{\partial p}{\partial r} = -\frac{Gm\rho}{r^2} + \mathcal{O}\left(\frac{1}{c^2}\right). \tag{3.2.2}$$

One could be tempted to make the assumption that $\frac{\partial p_{\text{TOV}}}{dr} \leq \frac{\partial p_{\text{LE}}}{dr}$. However this equation fails since the mass given in equation (3.1.24) is not the same as the one given in the LE equation. Using the previous relations for ρ and p and again setting $G = c = 1$, we can calculate

$$\frac{\partial p}{\partial r} = \frac{\partial}{\partial r}\left(K\rho^{1+1/n}\right) = K\lambda^{1+1/n}(n+1)\theta^n\frac{\partial\theta}{\partial r} = -\frac{m\lambda\theta^n}{r^2} \tag{3.2.3}$$

by using the definition of our polytropic EoS and equation (3.2.2). Rearranging and taking the derivative of this equation and using $\partial m/\partial r = 4\pi\rho r^2$, we obtain

$$-\frac{\partial m}{\partial r} = K\lambda^{1/n}(n+1)\frac{\partial}{\partial r}\left(r^2\frac{\partial\theta}{\partial r}\right) = -4\pi r^2\lambda\theta^n \tag{3.2.4}$$

Upon redefining $\xi = r/\kappa$ where $4\pi\kappa^2 = (n+1)K\lambda^{1/n-1}$, one can obtain the mathematically cleaner looking equation

$$\frac{1}{\xi^2}\frac{\partial}{\partial\xi}\left(\xi^2\frac{\partial\theta}{\partial\xi}\right) + \theta^n = 0 \tag{3.2.5}$$

Exact solutions are known for the cases $n = 0, 1, 5$. The derivation can be found in appendix A. Figure 2 and table 1 summarise them. Together with equation (3.2.5), we can already suspect that for values $n \geq 5$, the equation does not yield solutions with a zero value.

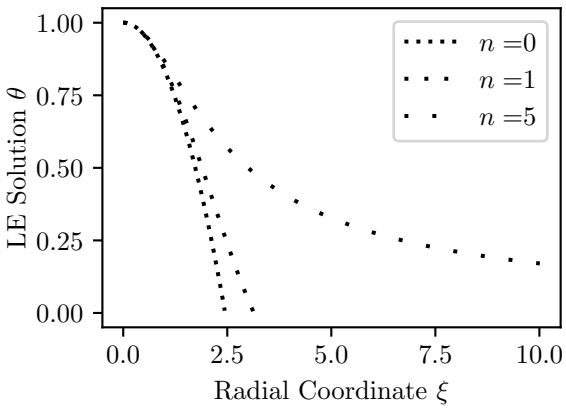

Figure 2: Graph of exact LE solutions.

n	LE Solution	ξ_0
$n = 0$	$1 - \frac{1}{6}\xi^2$	$\sqrt{6}$
$n = 1$	$\frac{\sin(\xi)}{\xi}$	π
$n = 5$	$\frac{1}{\sqrt{1+\frac{1}{3}\xi^2}}$	∞

Table 1: LE exact Solutions and their zero value.

3.3 Mass Bounds

We will first follow the approach given in [Wal84]. The first assumptions will be $d\rho/dr < 0$ and $\rho \geq 0$. Also we again consider a compact star, meaning $\rho(r) = 0$ for all $r > R$. We first state a useful Lemma for the proof of our next theorem.

Lemma 3.1
Given $\rho \in C^1(\mathbb{R}_{\geq 0})$ is monotonously decreasing, the function $\rho_{av} = m/r^3$ has negative slope.

Proof. Taking the derivative of ρ_{av} and applying equation (3.1.13), we obtain

$$\frac{\partial}{\partial r}\left(\frac{m}{r^3}\right) = -3\frac{m}{r^4} + \frac{4\pi\rho}{r}. \tag{3.3.1}$$

By equation (3.1.24) we know that p has negative slope and since ρ is monotonously increasing, we have

$$m = \int_0^r 4\pi\rho r^2 dr \geq \rho \int_0^r 4\pi r^2 = \frac{4\pi r^3 \rho}{3} \tag{3.3.2}$$

which shows that $\frac{4\pi\rho r^3}{3} \leq m$ and completes the proof. □

Theorem 3.2 - Mass Bound
The Mass of a spherically symmetric star is bound from above by

$$M < \frac{4}{9}R. \tag{3.3.3}$$

Proof. In our attempt to obtain an upper limit for the mass of a spherically symmetric star, we start by taking the difference of equation (3.1.11) and (3.1.12), we obtain

$$0 = \nu' \frac{e^{-\lambda}}{r} - \frac{1 - e^{-\lambda}}{r^2} - \frac{e^{-\lambda}}{2}\left[\nu'' + \left(\frac{\nu'}{2} + \frac{1}{r}\right)(\nu' - \lambda')\right] \tag{3.3.4}$$

$$= -\frac{2m(r)}{r^3} + \frac{\lambda' e^{-\lambda}}{2r} - \frac{e^{-\lambda}}{2}\left[\nu'' + \frac{\nu'^2}{2} - \frac{\nu'}{r} - \frac{\lambda'\nu'}{2}\right] \tag{3.3.5}$$

$$= r\frac{\partial}{\partial r}\left(\frac{m(r)}{r^3}\right) - \frac{e^{-\lambda}}{2}\left[\nu'' + \frac{\nu'^2}{2} - \frac{\nu'}{r} - \frac{\lambda'\nu'}{2}\right] \tag{3.3.6}$$

$$0 = \frac{\partial}{\partial r}\left(\frac{m(r)}{r^3}\right) - \frac{e^{-\lambda}}{2}\left[\frac{\nu''}{r} + \frac{\nu'^2}{2r} - \frac{\nu'}{r^2} - \frac{\lambda'\nu'}{2r}\right] \tag{3.3.7}$$

$$= \frac{\partial}{\partial r}\left(\frac{m(r)}{r^3}\right) - \frac{1}{2}e^{-\frac{\lambda+\nu}{2}}\frac{\partial}{\partial r}\left[\frac{1}{r}\nu' e^{\frac{\nu-\lambda}{2}}\right]. \tag{3.3.8}$$

Since $\partial_r \rho \leq 0$, also the average density $m(r)/r^3$ decreases with r. Thus we obtain

$$\frac{\partial}{\partial r}\left[\frac{1}{r}\nu' \exp\left(\frac{\nu - \lambda}{2}\right)\right] \leq 0. \tag{3.3.9}$$

We integrate this equation from R to $r < R$

$$\frac{\nu'}{r}\exp\left(\frac{\nu - \lambda}{2}\right) \geq \frac{2\nu'(R)}{R} e^{-\frac{1}{2}\lambda(R)} \left.\frac{\partial}{\partial r} e^{\frac{\nu}{2}}\right|_R \tag{3.3.10}$$

and use the Schwarzschild solution at $r = R$ for e^{λ} and e^{ν}. This is justified since we assumed $\rho(r) = 0$ for $r > R$ and thus we need to recover the vacuum solution for a spherically symmetric object which is given by the Schwarzschild solution. By continuity of the metric on every point of space, we can match

$$e^{-\lambda(r)}\big|_R = \left[1 - \frac{2M}{r}\right]_R = e^{\nu(r)}\big|_R \tag{3.3.11}$$

and with the explicit solution for $e^{-\lambda}$, we obtain

$$\left.\frac{2m(r)}{r}\right|_R = \frac{2M}{R}. \tag{3.3.12}$$

When plugging this into equation (3.3.11), the result is

$$\frac{\nu'}{2r}\exp\left(\frac{\nu-\lambda}{2}\right) \geq \frac{(1-2M/R)^{1/2}}{R}\,\frac{\partial}{\partial r}\left(1-\frac{2M}{r}\right)^{1/2}\Bigg|_{r=R} = \frac{M}{R^3}. \tag{3.3.13}$$

Now we multiply by $r\exp(\lambda/2)$ and use the explicit solution for e^{λ}

$$\frac{\partial}{\partial r}\left(e^{\frac{\nu}{2}}\right) \geq \frac{M}{R^3} r e^{\frac{\lambda}{2}} = \frac{M}{R^3}\left(r - 2m(r)\right) \tag{3.3.14}$$

and integrate again this time from 0 to R

$$e^{\nu(0)/2} \leq \left(1-\frac{2M}{R}\right)^{1/2} - \frac{M}{R^3}\int_0^R \left[1-\frac{2m(r)}{r}\right]^{-1/2} r\,dr. \tag{3.3.15}$$

As we have already noted, the average density $m(r)/r^3$ decreases, meaning explicitly $m(r)/r^3 \geq M/R^3$ and thus the integral with the previous equation can be written as

$$e^{\nu(0)/2} \leq \left(1-\frac{2M}{R}\right)^{1/2} + \frac{1}{2}\left[1-\frac{2Mr^2}{R^3}\right]^{1/2}\Bigg|_{r=0}^{r=R} = \frac{3}{2}\left(1-\frac{2M}{R}\right)^{1/2} - \frac{1}{2}. \tag{3.3.16}$$

The simple fact that $e^{\nu(0)/2} > 0$ then implies

$$\left(1-\frac{2M}{R}\right)^{1/2} > \frac{1}{3} \tag{3.3.17}$$

which is equivalent to

$$M < \frac{4R}{9}. \tag{3.3.18}$$

□

This shows that the mass of star has an upper limit under the assumptions $\rho \geq 0$, $\partial_r \rho \leq 0$ and $\rho(R) = 0$ for some $R \geq 0$.

4 Numerical Solutions

4.1 Comparing TOV and LE results with a polytropic EOS

In this section the numerical solutions of the TOV equation

$$\frac{\partial m}{\partial r} = 4\pi\rho r^2 \tag{4.1.1}$$

$$\frac{\partial p}{\partial r} = -\frac{m\rho}{r^2}\left(1+\frac{p}{\rho}\right)\left(\frac{4\pi r^3 p}{m}+1\right)\left(1-\frac{2m}{r}\right)^{-1} \tag{4.1.2}$$

as derived previously in section 3.1 will be discussed. To obtain numerical solvability a EoS in the form $\rho(r,p)$ is supplied. In Figure 3 a plot of such a solution is presented. The density ρ is derived via the equation (4.1.1) and the integration is done with a 4th order Runge-Kutta Method [Run95; Kut01; HSW10]. The integration is stopped once the pressure reaches values $p \leq 0$. The initial value of (4.1.1) is $\partial_r m(r=0) = 0$. For equation (4.1.1), the initial value can be calculated when applying L'Hôpital's rule and combining them to obtain

$$\lim_{r\to 0}\frac{m}{r} = \lim_{r\to 0}\frac{\partial m}{\partial r} = \lim_{r\to 0}\frac{4\pi\rho r^2}{1} = 0 \tag{4.1.3}$$

$$\lim_{r\to 0}\frac{m}{r^2} = \lim_{r\to 0}\frac{1}{2r}\frac{\partial m}{\partial r} = \lim_{r\to 0}\frac{4\pi\rho r^2}{2r} = 0 \tag{4.1.4}$$

$$\lim_{r\to 0}\frac{m}{r^3} = \lim_{r\to 0}\frac{1}{3r^2}\frac{\partial m}{\partial r} = \lim_{r\to 0}\frac{4\pi\rho r^2}{3r^2} = \frac{4\pi\rho_0}{3} \tag{4.1.5}$$

$$\lim_{r\to 0}\frac{\partial p}{\partial r} = 0 \tag{4.1.6}$$

Explicit code can be found in [Ple21]. The Lane-Emden equation was obtained in section 3.2 as the non-relativistic limit of the TOV equation by neglecting terms of order $1/c^2$ and higher and setting $G = c = 1$. To obtain numerical results for the LE equation as given in equation (3.2.5), a substitution of the form $d\theta/d\xi = \chi$ was used.

$$\frac{d\theta}{d\xi} = \chi \qquad \left.\frac{d\theta}{d\xi}\right|_{\xi=0} = 0 \tag{4.1.7}$$

$$\frac{d\chi}{d\xi} = -\frac{2}{\xi}\chi - \theta^n \qquad \left.\frac{d\chi}{d\xi}\right|_{\xi=0} = -\theta^n \tag{4.1.8}$$

where the initial value for $d\chi/d\xi$ can be calculated with L'Hôpital's rule. With the conversion factor κ derived in section 3.2, TOV and LE results can be compared. Figure 3 shows the solution of both equations for the parameters of table 2. Note that values in the last part are calculated instead of supplied to the solving routine. Additionally conversion equations to compare TOV and LE results are displayed.
Since the mass reads

$$m(r) = \int_0^r 4\pi r'^2 \rho(r')dr', \tag{4.1.9}$$

we expect $\partial m/\partial r(R) = 0$ if $p(R) = 0$ when choosing a polytropic equation of state with $\gamma > 0$. The plot in figure 3 shows this expected behaviour for the Lane Emden equation at $r \approx 2.31$ and has the same behaviour for the TOV results at $r \approx 6.80$.[3]

[3]For the purpose of nicely displaying the calculated result, the plot only shows result up to $r = 2.5$

TOV		**LE**	
EOS	$\rho = Ap^{1/\gamma}$	EOS	$p = K\rho^{\gamma}$
A	2		
$\gamma = 1 + \frac{1}{n}$	$4/3$	$n = 1/(\gamma - 1)$	3
p_0	0.5	θ_0	1
m_0	0	$d\theta_0$	0
dr	0.01	$d\xi = dr/\kappa$	$0.01/0.3355 \approx 0.0298$
$\rho_0 = Ap_0^{1/\gamma}$	$2(2)^{\frac{4}{3}} \approx 1.1892$	$\lambda = \rho_0$	$2(2)^{\frac{4}{3}} \approx 1.1892$
		$K = A^{-1/\gamma}$	$2^{-3/4} \approx 0.5946$
		$\kappa^2 = ((n+1)K\lambda^{1/n-1})/(4\pi)$	≈ 0.1125

Table 2: Numerical Parameters for TOV and LE equation.

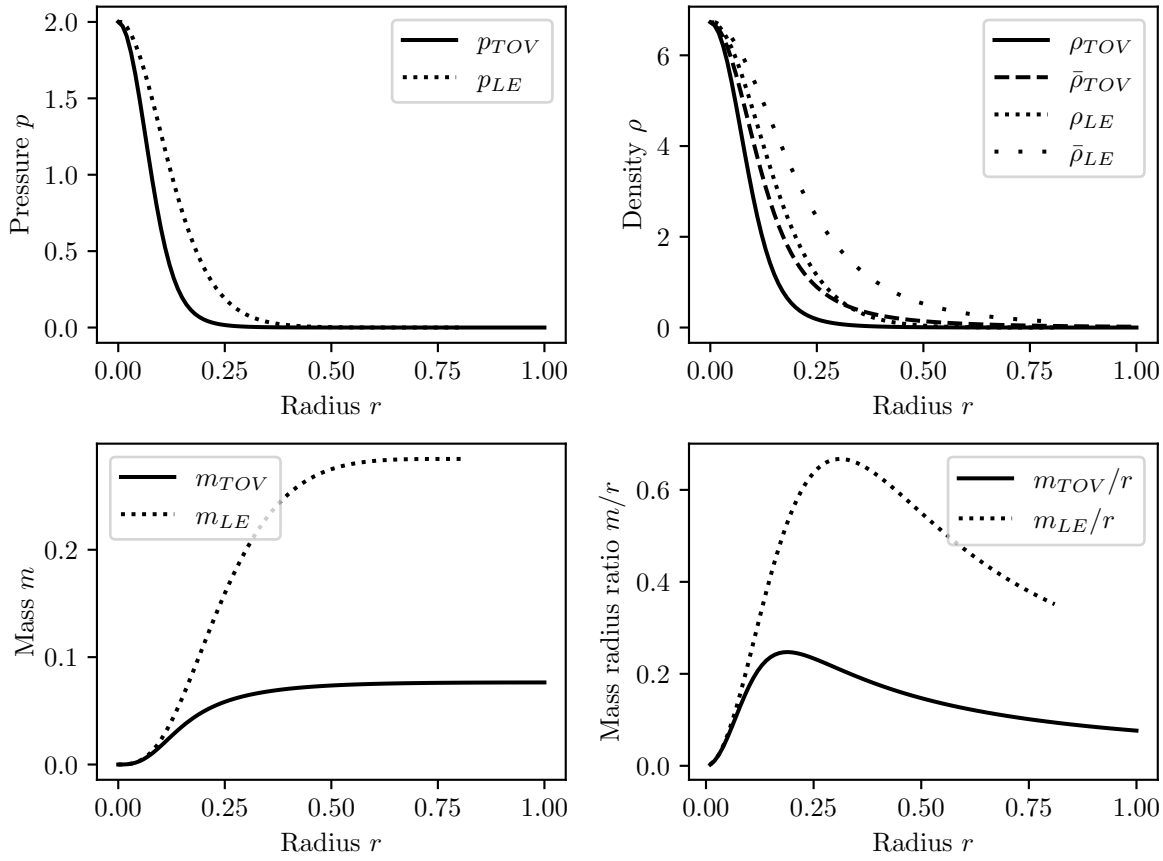

Figure 3: Comparison of the general relativistic TOV result with polytropic EoS to the classical Lane-Emden solution. The images show the plots for the parameters of table 2. First the pressure is presented. Afterwards the density calculated with the given EOS and the average density $\bar{\rho}_i = (4\pi/3)^{-1} m_i/r^3$ for the two solutions are beeing compared. In the second row, the mass and the ratio m_i/r can be seen.

4.2 Verifying the results

One can compare calculated LE results with already known exact solutions for certain exponents as given in table 1. All calculations are carried out with a chosen step size of $d\xi = 0.03$.
The graphs overall show good numerical agreement. Initial values at $r = 0$ are identical since they were set to be. The spike occurring afterwards can be explained by equation (4.1.8). The initial value of all derivatives is identically 0 which means no change of value for θ or χ for the initial step of the numerical integration. On the other hand the exact results will see a change which explains the large discrepancy in the beginning. It is clear that the relative difference on the right hand side will spike again once smaller values for θ are reached if the absolute difference stays constant. This behaviour is best seen in the solution for $n = 5$ where a large range of $0 \leq r \leq 100$ for solving was chosen. The offset between the numerically calculated values and the exact result stays constant while the value of θ decreases inverse proportionally. Despite this behaviour we can see that the criterion for convergence is fulfilled in the last column of figure 4.

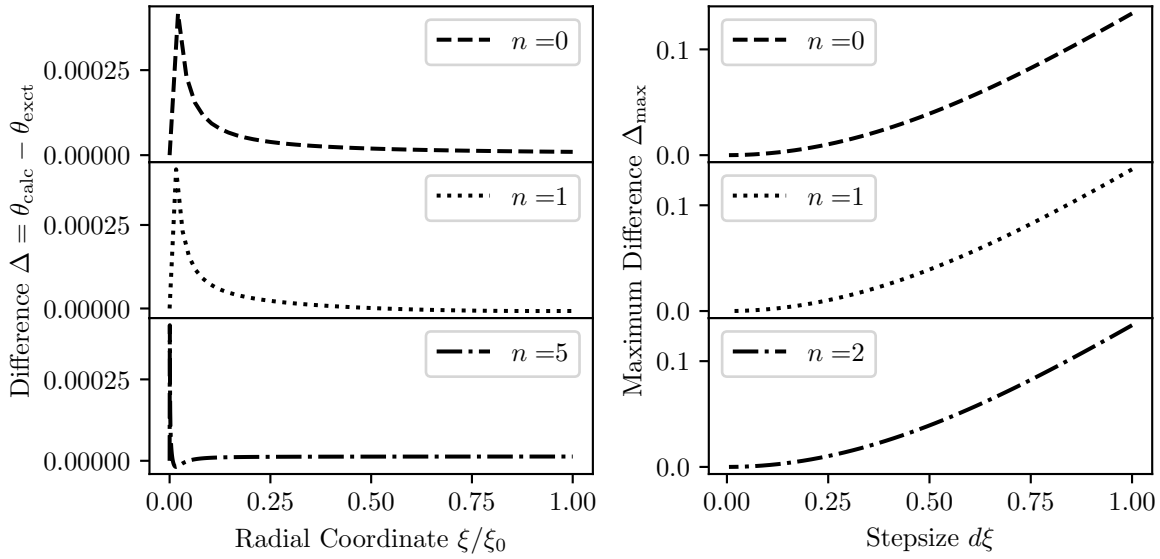

Figure 4: Validation of numerical LE results - The first two plots show absolute and relative difference of known exact and numerically calculated results while the third plot shows the behaviour of the maximum value of Δ as the stepsize decreases.

As can be seen in the last column of plots, the condition for convergence in this case is well fulfilled. The double logarithmic plot displays nicely that by lowering the integration stepsize, the maximum difference in this inverval decreases.

4.3 Relativistic EOS

In the previous discussion, we relied on the EOS given in table 2. This is a versatile assumption, but one could ask, what would happen to a star in which the particles have no interaction but are near relativistic speed. The resulting EOS was calculated in the beginning (see equation (2.3.26)) although not written down explicitly. Since explicit inversion of the given function is hard, we rely on numerical methods for calculation.

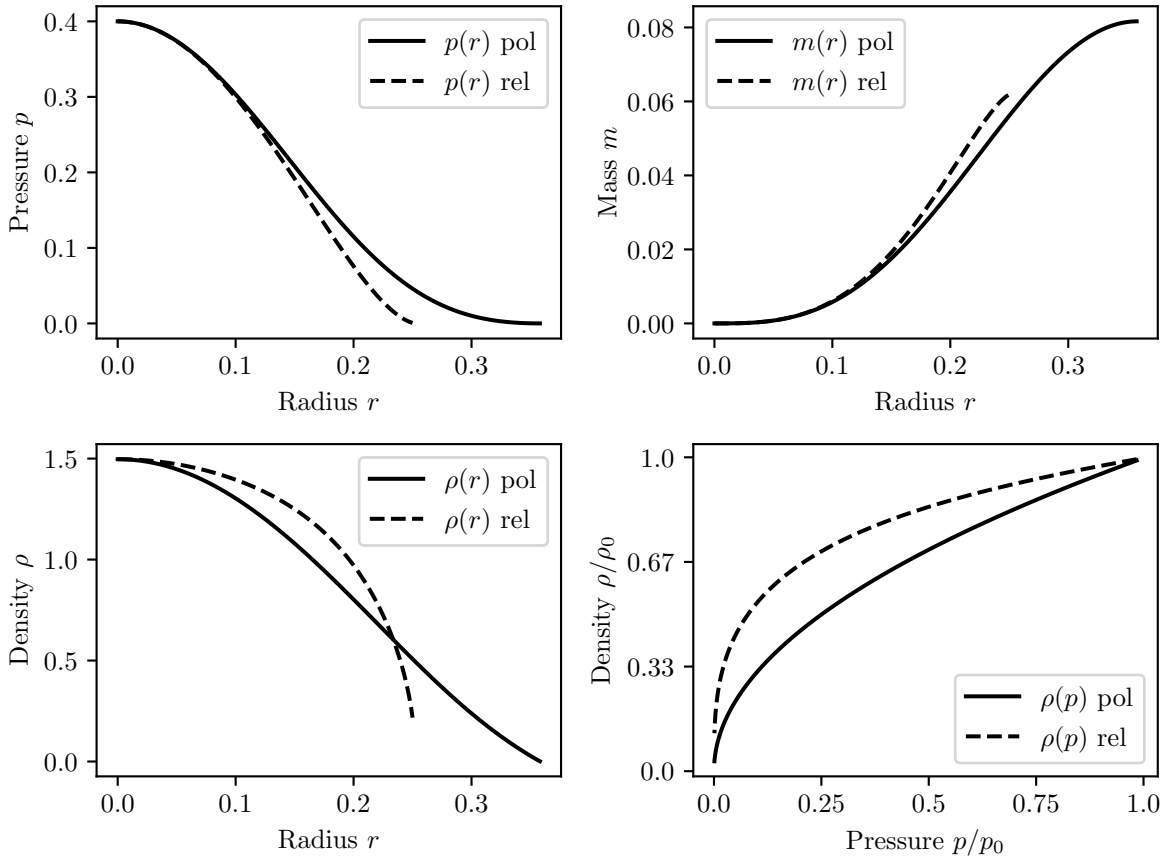

Figure 5: Comparison of TOV polytropic and relativistic EoS

Section 2.3 showed that the function given in equation (2.3.11)

$$p(\alpha) = CNmc^2 \frac{1}{K_2(\alpha)\alpha^2} \exp\left(-\alpha \frac{K_1(\alpha) + K_3(\alpha)}{2K_2(\alpha)}\right). \tag{4.3.1}$$

explicitly has a non-positive slope. When calculating a inverse function the values C, N, m need to be chosen high enough in order to reach sufficiently high values for p. By knowing the initial value p_0 and by the fact that the TOV solution pressure (3.1.22) has non-positive slope and with equation (2.3.12), it is sufficient to choose $Bp_0 = CNmc^2 > 2/e^2$. On the other hand it is also important to choose high enough values for α for numerical inversion since otherwise functions can not be displayed if they reach small enough values for p. The limit for α is chosen such that values as low as $0.001p_0$ can be evaluated. Afterwards the function over the given interval is inverted by a polynomial fit and then used in equation (2.3.10) to obtain the EoS.
Figure 5 is an example which shows a clear difference between the polytropic and relativistic EoS. The values used are $B = 20$, $p_0 = 0.4$, $dr = 0.001$, $n = 1$. The correct prefactor A of the polytropic EoS is chosen after numerical calulation of the relativistic EoS. It is then simply given by

$$A = \frac{\rho_{\text{rel}}(p_0)}{p_0^{1/\gamma}}. \tag{4.3.2}$$

This normalises both EoSs to same inital pressures.

4.4 Zero Values of the TOV and LE equation

Having discussed individual solutions for the TOV and LE equation, this section now turns to analysing zero values of both equations. We define a zero value as the first point in which the solution of our differential equation reaches value 0, or more precisely where the pressure p reaches zero.[4] Even now the problem is not well posed since for different solving routines alternative transformations may be used. This has to be kept in mind when comparing results. Apart from the previously defined exact solutions of table 1 we will only use the parameter r as defined by equation (3.1.24) to display final results. In order to solve the equations, a transformation in the form applied in section 3.2 is used since it was hoped to increase the precision with which the zero value is determined. This can be motivated by looking at plots for LE solutions as in figure 2 and comparing them to TOV results of figure 3. With the EoS $\rho = Ap^{1/\gamma}$ and the new definition $\rho = \rho_0\theta^n$, the equations used are

$$\frac{\partial m}{\partial \xi} = \quad 4\pi\kappa^3\rho\xi^2 \tag{4.4.1}$$

$$\frac{\partial \theta}{\partial \xi} = -\frac{\left(1 + K\rho_0^{1/n}\theta\right)\left(4\pi\xi^3\kappa^3 K\rho_0^{1+1/n}\theta^{n+1} + m\right)}{\left((n+1)K\rho_0^{1/n}\kappa\xi^2\right)\left(1 - \frac{2m}{\kappa\xi}\right)} \tag{4.4.2}$$

where $\rho = \rho_0\theta^n$ and initial values $\partial m/\partial\xi = 0$ and $\partial\theta/\partial\xi = 0$ can again be calculated with L'Hospitals rule and $\theta_0 = 1$ together with $m_0 = 0$. When comparing equations (4.4.2) and (3.1.24) one can immediately recognise the distinct terms. When talking about zero values we stated earlier that transformations need be accounted for when comparing results. However in this case since

$$p = \frac{\rho_0^n\theta^n}{A^{1+1/n}} \tag{4.4.3}$$

it is clear that a zero values of θ and p match under the same parameter ξ. When transforming back by using $\kappa\xi = r$ as explained in section 3.2 one should note that κ depends on n via

$$4\pi\kappa^2 = (n+1)K\rho_0^{1/n-1} \tag{4.4.4}$$

and it will thus change values by more than constant scaling. Figure 6 shows zero values for solutions of the TOV and LE equations respectively with their dependence on n. Since not only the parameters A and n in the EoS may alter results but also the initial value p_0 a family of curves was plotted. The upper half of the plot displays a currently not explainable bump which is prominent in the TOV $p_0 = 0.1$ case. A similar but dampened behaviour can also be seen along the $p_0 = 1$ curve. It is unclear if the TOV solutions just like the LE blow up at the same combination of parameters. This observation motivates to state a theorem that for every combination of parameters A, p_0 there exists a value n_0 such that each solution of the TOV equation has no zero values for that particular combination of parameters A, p_0 if $n \geq n_0$. The methods to prove this theorem will be discussed in the next section.
In figure 6 every point on a line represents solving the differential equation until the pressure reaches its zero value. Numerical optimisations to speed up calculation times and a short discussion on the methods used can be found in the appendix in section D.

[4]Note that p_0 still denotes the initial value while r_0 and ξ_0 denote values where $p = 0$.

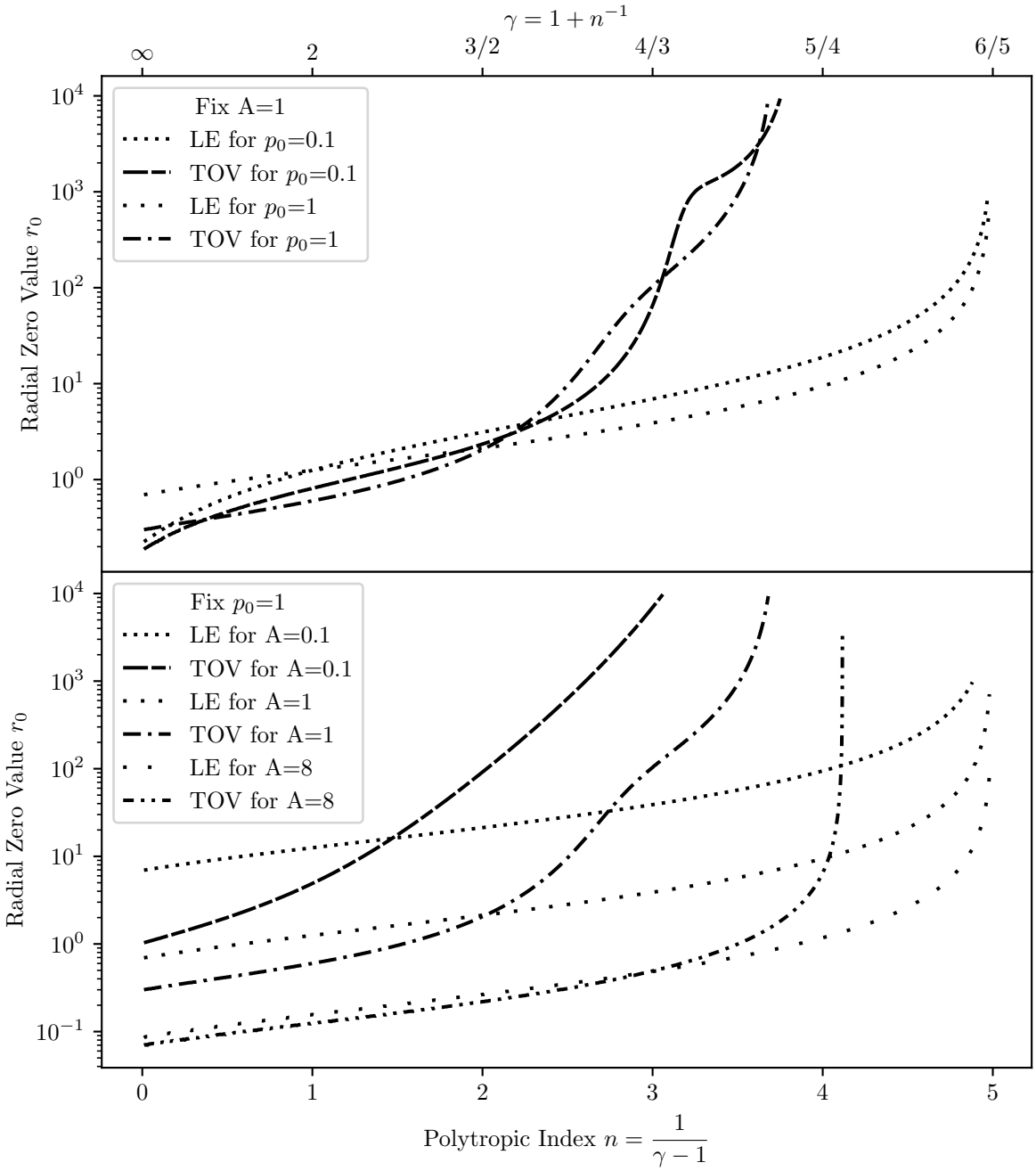

Figure 6: Zero Values of TOV and LE equation - In the first plot results for $p_0 = 8$ have been omitted for better visual clarity. These behave similar to the $p_0 = 1$ results.

5 To a General Zero Value Theorem

5.1 LE Equation

Motivated by the preceding sections, the aim now is to prove the following theorem.

Theorem 5.1 - Lane-Emden Finite Boundary
For every $0 \leq n < 5$, the Lane-Emden equation

$$\frac{1}{\xi^2}\frac{d}{d\xi}\left(\xi^2\frac{d\theta}{d\xi}\right) + \theta^n = 0 \tag{5.1.1}$$

with $\theta_0 = 1$ has a zero value for a finite ξ_0. To prove this theorem, show the statements 5.2, 6.1 and 6.2.

We explain what the idea behind the proof is. ...

Lemma 5.2 - LE Local Existence
For every $n \geq 0$, the Lane-Emden equation 5.1.1 with initial values defined as above has a unique solution in an ϵ Ball around $\xi = 0$.

With the aid of the Picard-Lindelöf theorem or the

Proof. This proof can be generalised to $l \geq 2$ dimensions. Following [QS07] we see that the LE differential equation can be written as

$$\frac{d}{d\xi}\left(\xi^{l-1}\frac{d\theta}{d\xi}\right) + \xi^{l-1}\theta^n = 0. \tag{5.1.2}$$

Integrating once and rearranging leads us to

$$\frac{d\theta}{d\xi} = \left.\frac{d\theta}{d\xi}\right|_0 - \int_0^\xi \left(\frac{t}{\xi}\right)^{l-1}\theta^n dt. \tag{5.1.3}$$

By choosing the correct initial value[5] of $d\theta/d\xi = 0$ we see that positive solutions to the LE equation need to have negative slope. This equation also shows that for $\theta_0 > 0$, the solution θ will be positive in a ϵ region around $\xi = 0$. We integrate both sides again and end up with

$$\theta = \theta_0 - \int_0^\xi \int_0^s \left(\frac{t}{s}\right)^{l-1}\theta^n dt ds. \tag{5.1.4}$$

We define C^* as the space of all real continuous functions $f \geq 0$ on $[0, \epsilon]$ that share the same initial value θ_0 and with non-positive slope. Additionally with equation (5.1.3) we can restrict ourselves to functions with

$$\frac{d\theta}{d\xi} \geq -\theta_0^n\frac{\xi}{m}. \tag{5.1.5}$$

[5] One has to choose this value in order to obtain the correct limiting case when using the non-relativistic limit of the TOV equation. See also section 3.2

With the norm $||.||_\infty$ this space is complete. Inspecting the operator $T : C^* \to C^*$ defined by equation 5.1.4 we can apply the Banach fixed-point theorem [Ban22].

$$||T(U) - T(V)||_\infty \leq ||U^n - V^n||_\infty \int_0^\xi \int_0^s \left(\frac{t}{s}\right)^{l-1} dtds \tag{5.1.6}$$

$$= ||U^n - V^n||_\infty \frac{\xi^2}{2l} \tag{5.1.7}$$

Let $n \geq 1$. Since the function $x \mapsto x^n$ is differentiable for $n \geq 1$ it is also Lipschitz with constant L on the compact interval $I = [0, \theta_0]$. This means in particular that we have

$$||T(U) - T(V)||_\infty \leq ||U - V||_\infty \frac{L\xi^2}{2l} \tag{5.1.8}$$

Thus when choosing $\epsilon < \sqrt{2m/L}$ we have a contraction and the Banach fixed-point theorem then gives us a unique solution to equation 5.1.4.
Now let $0 \leq n < 1$. In this situation the preceding method does not work due to x^n not being differentiable or Lipschitz at $x = 0$. Since by definition of C^*, we had chosen (5.1.5) as an additional constraint, we can now choose ϵ small enough to have $\theta \geq q > 0$ on $[0, \epsilon]$. Then the same procedure as before can be carried through but with the interval $I = [q, \theta]$. □

Equation (5.1.3) shows that non-negative solutions must have non-positive slope. The following theorem makes use of that fact and of a different representation of the LE equation to show that solutions can be extended until they reach zero.

Lemma 5.3
Let θ be a LE solution on $[0, \epsilon)$. Additionally suppose that $\lim_{\xi \to \epsilon} \theta(\xi) > 0$. Then we can find a δ such that an extension of θ around ϵ exists.

Proof. First we will rewrite the LE equation.

$$\frac{d\theta}{d\xi} = \chi \tag{5.1.9}$$

$$\frac{d\chi}{d\xi} = -\theta^n - \frac{2}{\xi}\chi \tag{5.1.10}$$

From here we can see that this equation at $\epsilon > 0$ is solvable by means of the Picard-Lindelöf theorem.

□

5.2 TOV Equation

6 Ideas

Theorem 6.1 - Lane-Emden Finite Boundary 2
For $n < 5$, the Lane-Emden equation 5.1.1 has no Solution defined on the total space $\mathbb{R}_{\geq 0}$.

Proof. From [QS07] we know that solutions for equation 5.1.1 on the total space exist for $n \geq 5$.

□

Theorem 6.2 - Lane-Emden Finite Boundary 3
Let $n < 5$ and $\theta : [0, x) \to \mathbb{R}$ be a solution of 5.1.1. If $\theta(x) > 0$, then θ can be extended with Theorem 5.2 to $[0, x + \epsilon)$ where ϵ follows a growth condition $\epsilon(\xi) = ...$ such that if θ would have no zero point, there would be a solution on total $\mathbb{R}_{\geq 0}$ and thus a contradiction with 6.1.

Theorem 6.3 - Lane-Emden Finite Boundary 4
The Lane Emden equation has a zero value if the exponent function $n(\xi)$ fullfills the growth condition XYZ.

Theorem 6.4 - TOV Finite Boundary
For each $A > 0$, the TOV equation 4.1.1 has a exponent $n > 0$ for which a solution p does not have any zero points.

Theorem 6.5 - TOV Finite Boundary 1
If p_1 and p_2 are two solutions of the TOV equation (for equal A) with p_i corresponding to n_i exponents, then if $n_1 < n_2$, the zero point (if it exists) of p_1 is smaller than that of p_2 (if it exists or is ∞).

Theorem 6.6 - TOV Finite Boundary 2
a

7 Outlook

Appendix

A Known Exact Solutions of the LE Equation

This section relies on information in [Wei20] and [Cha58]. The LE equation is

$$\frac{1}{\xi^2}\frac{d}{d\xi}\left(\xi^2\frac{d\theta}{d\xi}\right)+\theta^n=0 \tag{A.1}$$

which for $n=0$ transforms readily into

$$\int_0^\xi \frac{d}{d\xi}\left(\xi'^2\frac{d\theta}{d\xi}\right)d\xi' = -\int_0^\xi \xi'^2 d\xi'. \tag{A.2}$$

Both sides can be evaluated directly and then simplified further.

$$\xi^2\frac{d\theta}{d\xi} = -\frac{\xi^3}{3} \tag{A.3}$$

$$\theta(\xi) = \theta(0) - \frac{\xi^2}{6} \tag{A.4}$$

With the initial condition $\theta(0)=1$, we obtain the desired result. For $n=1$, equation A.1 transforms into

$$\frac{d}{d\xi}\left(\xi^2\frac{d\theta}{d\xi}\right)+\xi^2\theta=0 \tag{A.5}$$

we start by substituting $U=\theta x$ and thus obtain (also multiplying by x^2)

$$0 = \frac{dU}{d\xi}+\xi\frac{d^2U}{d\xi^2}-\frac{dU}{d\xi}+\xi U \tag{A.6}$$

$$-U = \frac{d^2U}{d\xi^2} \tag{A.7}$$

and the last equation can be solved with a linear combination of $\cos(\xi)$ and $\sin(\xi)$. Transforming back to θ, we then have

$$\theta(\xi) = A\frac{\sin(\xi)}{\xi} - B\frac{\cos(k\xi)}{\xi}. \tag{A.8}$$

The need for a well defined limit at $\xi\to 0$ implies that $B=0$ and thus since $\sin(z)/z\to 1$ for $z\to 0$, we have $A=\theta(0)=1$ and

$$\theta(\xi) = \frac{\sin(\xi)}{\xi}. \tag{A.9}$$

For $n=5$, we start by making the two substitutions $x=1/\xi$ and $\theta=ax^\omega$ as done in [Cha58, pp. 94 sqq.] and then transforming the LE equation into

$$x^4\frac{d\theta}{d\xi} + \theta^n = 0 \tag{A.10}$$

$$a\omega(\omega-1)x^{\omega+2} + a^n x^{n\omega} = 0. \tag{A.11}$$

From this we see that $\omega + 2 = n\omega$ and $a\omega(\omega - 1) = -a^n$ needs to be satisfied, since the equation needs to hold for all $x \in \mathbb{R}_{\geq 0}$. Rewriting these conditions, we obtain the singular solution for the LE equation

$$\theta(x) = \left(\frac{2(n-3)}{(n-1)^2}\right)^{1/(n-1)} x^{2/(n-1)} \tag{A.12}$$

since with $x = 1/\xi$, we have $\theta(\xi) \to \infty$ for $\xi \to 0$. Notice that the solution is only valid if $n \geq 3$. We can use this solution to the LE equation and perturb it to make the more general ansatz

$$\theta(x) = ax^{\omega} z(x). \tag{A.13}$$

If $n < 3$, the factor a has to be replaced with a more general one. The singular solution is obtained when taking $z = 1$. Using another transformation $1/x = \xi = \exp(-t)$, we obtain

$$\frac{1}{\xi^2}\frac{d}{d\xi}\left(\xi^2 \frac{d\theta}{d\xi}\right) + \theta^n = 0 \tag{A.14}$$

$$x^4 \frac{d^2\theta}{dx^2} + \theta^n = 0 \tag{A.15}$$

$$ax^{\omega+2}\left[x^2\frac{d^2z}{dx^2} + 2\omega x\frac{dz}{dx} + \omega(\omega-1)z\right] + a^n x^{n\omega} z^n = 0 \tag{A.16}$$

$$\frac{d^2z}{dt^2} + (2\omega - 1)\frac{dz}{dt} + \omega(\omega-1)z + a^{n-1}z^n = 0 \tag{A.17}$$

$$\frac{d^2z}{dt^2} + \frac{5-n}{n-1}\frac{dz}{dt} + 2\frac{3-n}{(n-1)^2}z + 2\frac{(n-3)}{(n-1)^2}z^n = 0. \tag{A.18}$$

For $n = 5$, we obtain

$$\frac{d^2z}{dt^2} = \frac{1}{4}z(1 - z^4). \tag{A.19}$$

we multiply both sides with dz/dt and integrate

$$\frac{1}{2}\left(\frac{d^2z}{dt^2}\right) = \frac{1}{8}z^2 - \frac{1}{24}z^6 + D \tag{A.20}$$

where D is the integration constant. For $\xi \to 0$, we expect $\theta \to \theta_0$ and thus $z = \theta_0 e^{-\omega t}(1/a + \mathcal{O}(e^{-t}))$ as t approaches ∞. We immediately see that dz/dt exhibits a similar behaviour and thus the integration constant D has to vanish.
The right hand side of equation A.20 cannot get negative since otherwise z would take complex values which enables us to take the square root with a minus sign[6] and integrate again

$$\int \left(1 - \frac{1}{3}z^4\right)^{-1/2} \frac{dz}{z} = -\frac{1}{2}\int dt. \tag{A.21}$$

We change the integration by again substituting the variables $1/3z^4 = \sin^2(\alpha)$ and calculate $dz/z = 2\cos(\alpha)/\sin(\alpha)d\alpha$ as well as $-dt = d\alpha/\sin(\alpha)$. Now we rewrite the integral

$$\int \frac{1}{\sqrt{1 - \sin^2(\alpha)}} \frac{2\cos(\alpha)}{\sin(\alpha)} \frac{d\alpha}{} = -\int dt \tag{A.22}$$

$$\int \frac{2d\alpha}{\sin(\alpha)} = -\int dt. \tag{A.23}$$

[6]This only determines the direction in which t is defined, so it is arbitrary.

Evaluating those integrals leads us to

$$\log(\tan(\alpha/2)) + \log(1/C) = -t \tag{A.24}$$

where the integration constant has been chosen in advance to simplify the next expressions. From here, we further manipulate equation A.24 and combine it with our previous substitution $1/3z^4 = \sin^2(\alpha)$ to obtain

$$\frac{1}{3}z^4 = \sin^2(\alpha) = \frac{4\tan^2(\alpha/2)}{(1+\tan^2(\alpha/2))}^2 \tag{A.25}$$

and with the solution for out integral before and plugging in the substitution from the beginning $\xi = e^{-t}$, we have

$$z = \pm\left(\frac{12C^2\xi^2}{1+C^2\xi^2}\right)^{1/4}. \tag{A.26}$$

For θ, we need to have $\theta \to \theta 0 = 1$ as $\xi \to 0$. This means that $C = 1$ and with $\theta = ax^\omega z$, we obtain

$$\theta = \frac{1}{\left(1+\frac{1}{3}\xi^2\right)^{1/2}}. \tag{A.27}$$

We see that this equation has no zero value and tends to 0 as $\xi \to \infty$.

B New Exact LE Series Solution at Index 2

One can derive another exact solution for the LE equation at the exponent $n = 2$ when considering a series expansion of θ around the point $\xi = 0$ with initial conditions

$$\theta = \sum_{m=0}^{\infty} a_m \xi^m \qquad a_0 = \theta|_{\xi=0} = \theta_0 \qquad a_1 = \left.\frac{d\theta}{d\xi}\right|_{\xi=0} = 0 \tag{B.1}$$

Since the series is absolut convergent, we can plug it into the LE equation 3.2.5 and use the Cauchy Product formula.

$$\sum_{m=2}^{\infty} m(m-1)a_m\xi^{m-2} + \sum_{m=1}^{\infty}(2m)a_m\xi^{m-2} + \sum_{m=0}^{\infty}\sum_{k=0}^{m} a_{m-k}a_k\xi^m = 0 \tag{B.2}$$

Theorem B.1
The odd coefficients a_{2m+1} of this series expansion vanish.

Proof. We rewrite the summations of equation B.2 to start at the same index $m = 0$ and combine them

$$\sum_{m=0}^{\infty}\left((m+2)(m+1)a_{m+2}\xi^m + (2m+2)a_{m+1}\xi^{m-1} + \sum_{k=0}^{m} a_{m-k}a_k\xi^m\right) = 0 \tag{B.3}$$

With equation B.1, we can start the summation in the middle one index higher and separate the term ξ^m. This equation has to be true inside the radius of convergence of the series and thus needs to vanish for ambiguous ξ.

$$(m+2)(m+1)a_{m+2} + 2(m+2)a_{m+2} + \sum_{k=0}^{m} a_{m-k}a_k = 0 \tag{B.4}$$

and upon further manipulation results in the recursive description for the coefficients of the series

$$a_{m+2} = -\frac{1}{(m+2)(m+3)} \sum_{k=0}^{m} a_{m-k} a_k. \tag{B.5}$$

We show the statement by induction. For a_1 it is already true. Let the statement be true for all odd values $2k+1 \leq 2m+1$. Writing down a_{2m+3} gives us

$$a_{2m+3} = -\frac{1}{(2m+3)(2m+4)} \left(a_0 a_{2m+1} + a_1 a_{2m} + \cdots + a_{2m} a_1 + a_{2m+1} a_0 \right). \tag{B.6}$$

It is clear that in the summation odd and even coefficients get paired and will thus vanish completely. □

This proof shows that we can restrict ourselves to the subsequence $b_m = a_{2m}$ and the subseries with initial values given by

$$\theta = \sum_{m=0}^{\infty} b_m \xi^{2m} \qquad b_{m+1} = -\frac{1}{(2m+2)(2m+3)} \sum_{k=0}^{m} b_{m-k} b_k \qquad b_0 = \theta_0 \tag{B.7}$$

Theorem B.2
The series $\theta = \sum_{m=0}^{\infty} b_m \xi^{2m}$ converges for $\xi \leq 1$.

Proof. We start by showing that $|b_{m+1}| \leq 1/(4m+6)$. Using the triangle inequality on B.7, we obtain

$$|b_{m+1}| \leq \frac{1}{(2m+2)(2m+3)} \sum_{k=0}^{m} |b_{m-k} b_k|. \tag{B.8}$$

For $m = 0$, we have $b_1 = -1/6$ and thus $|b_1| \leq 1/3$ and so the statement is true for $m = 0$. If the statement holds for all $m < m+1$, we have

$$|b_{m+1}| \leq \frac{m}{(2m+2)(2m+3)} = \frac{1}{2} \frac{m}{(m+1)} \frac{1}{(2m+3)} \leq \frac{1}{2} \frac{1}{(2m+3)} \tag{B.9}$$

which proves the first statement. To see that b_m is a alternating sequence, we again inspect B.7. The first element of the series is $b_0 = 1$ and the second is $b_1 = -1/6$ so the initial statement is again correct. Let b_m be alternating for all $m < 2m+1$. Then equation B.7 for odd values reads

$$b_{2m+1} = -\frac{1}{(4m+4)(4m+5)} \left(b_{2m} b_0 + b_{2m-1} b_1 + \cdots + b_0 b_{2m} \right) \tag{B.10}$$

This shows that if all odd values b_{2k+1} are negative and all even ones are positive, then b_{2m+1} is negative too. The same holds true when the index $2m+2$ is even. By the Leibniz criterion the series converges if $\xi \leq 1$. □

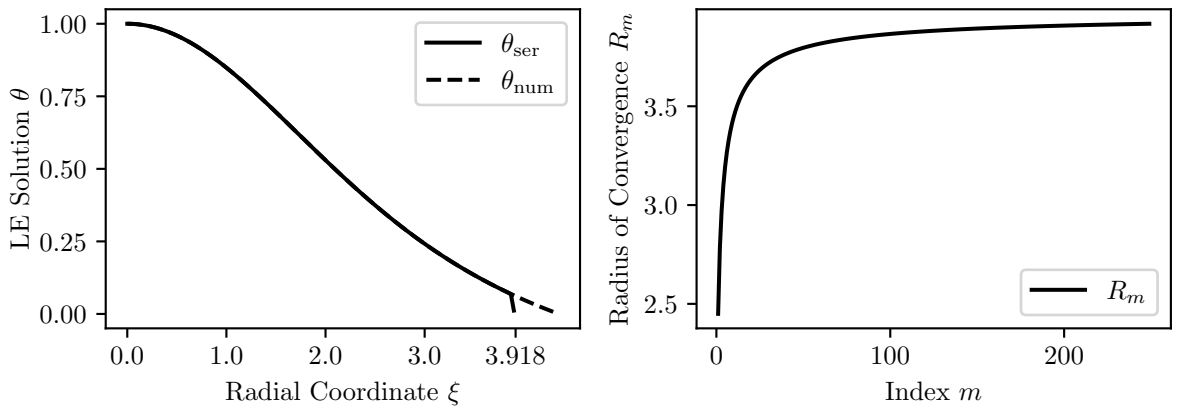

Figure 7: LE Solution for $n = 2$ - We see the power the series calculated with the coefficients explained above (the far right tick is the last calculated value for R_m where plotting is stopped) and the sequence $R_m = (|a_m|)^{-1/m}$ which approaches the radius of convergence.

These results can be used to calculate the power series of the LE equation numerically. Figure 7 shows those results. Good agreement is found between the two solutions as the difference $\Delta = \theta_{calc} - \theta_{ser}$ is not larger than 0.00015. The solutions differ for larger values around ≈ 3.918 The top right plot indicates that the radius of convergence might actually be larger than where solutions deviate. One important observation is that in this procedure, the coefficients were calculated up to $b_{250} \approx -4.7723 \times 10^{-296}$ which is in close proximity to the floating point limit of python given by $\approx 2.2251 \times 10^{-308}$ and indicates that numerical errors may be the reason the series starts to diverge. Also in order to achieve sufficient numerical precision, we would need to calculate higher order terms of the series, which is supported by $(R_{250})^{500} \approx 3.2159 \times 10^{296}$ and shows that these parts of the series still yield large contributions to the value of θ at this point.

C Exact TOV Solution in Absence of Mass

Theorem C.3 - TOV Exact Solution
The TOV equation 4.1.1 with a polytropic EOS $\rho = Ap^{1/\gamma}$ has a well defined limiting case where $A \to 0$ with $m = 0$ and

$$p = \frac{p_0}{2\pi r p_0 + 1} \tag{C.1}$$

Proof. First we transform the TOV equation 3.1.24 using $p = y^a$ with $a > 0$ and $m = Arv$ and together with the polytropic EOS $\rho = Ap^{1/\gamma}$ obtain

$$\frac{\partial v}{\partial r} = 4\pi r y^{a/\gamma} - Av \tag{C.2}$$

$$a y^{a-1} \frac{\partial y}{\partial r} = -\frac{vA^2 y^{a/\gamma}}{r} \left(1 + \frac{y^a}{Ay^{a/\gamma}}\right) \left(\frac{4\pi r^2 y^a}{Av} + 1\right) \frac{1}{1 - 2vA} \tag{C.3}$$

Rearranging the second equation one obtains

$$\frac{\partial y}{\partial r} = -\frac{y^{a/\gamma - a + 1}}{ar} \left(A + y^{a - a/\gamma}\right) \left(4\pi r^2 y^a + Av\right) \frac{1}{1 - 2vA}. \tag{C.4}$$

Using $\gamma = 1 + 1/n$ with $n > 0$, we see that this equation is continuous in every variable $(r, y, v) \in \mathbb{R}_{>0} \times \mathbb{R}_{\geq 0} \times [0, 1/2A)$. We restrict ourselves to a compact domain $r \in \overline{B_\delta(\tau)}$ and $v \in [0, 1/2A - \epsilon]$ where $0 < \epsilon < 1/2A$. We choose $0 < \delta$ and $0 \leq \tau$ in such a way that $0 < \epsilon < 1/2A$ is satisfied for some ϵ which is possible since $m \to 0$ for $r \to 0$. To obtain Lipschitz continuity in (y, v), all of the following conditions need to be fulfilled.

$$\frac{a}{\gamma} - a + 1 \geq 1 \qquad a - \frac{a}{\gamma} \geq 1 \qquad a \geq 1 \tag{C.5}$$

The second equation implies the first and the third. Thus we only need to choose $a \geq (1 - 1/\gamma)^{-1}$. With $\gamma = 1 + 1/n$ we can rewrite this equation to

$$a \geq n + 1 \tag{C.6}$$

which can be easily satisfied. This now shows with extension of the Picard-Lindelöf Theorem that there exists a unique solution for given initial values $\tau, y(\tau), v(\tau) \in B_\delta(\tau) \times \mathbb{R}_{\geq 0} \times [0, 1/2A - \epsilon)$ that especially continuously depends on A. Without loss of generality we can choose δ small enough such that solutions are positive in p. By transforming back equation C.3 to

$$\frac{\partial p}{\partial r} = -\frac{1}{r^2}\left(Ap^{1/\gamma} + p\right)\left(4\pi r^3 p + vA\right)(1 - 2vA)^{-1} \tag{C.7}$$

and letting $A \to 0$, we obtain

$$\frac{\partial p}{\partial r} = -4\pi r p^2 \tag{C.8}$$

which is then solved by

$$p = \frac{\tilde{p}}{2\pi\tilde{p}(r^2 - \tau^2) + 1} \tag{C.9}$$

where $\tilde{p}$ is the initial value at $r = \tau$. It is clear that this solution can be extended to $r \in [0, \infty)$ by choosing arbitrary small τ. In the limit, the result equals the hypothesis. □

D Numerical Optimisations

When solving the TOV or LE equation numerically calculations for the next step clearly depend on results from the before calculated one. This simple fact which is integral to the concept of an Ordinary Differential Equation (ODE) means that numerics is single thread [7] bound which already puts one at a systematic disadvantage. This means any effort to parallelise the given task must focus on distributing the individual solving routines to respective threads. With this first consideration at hand a server with high number of processing units may come into mind to then speed up the calculation. However in the situation of section 4.4 this would only allow us to calculate more results in parallel but not speed up the individual solving routines. And this is exactly the bottleneck in our case. When looking at figure 6 it is clear that higher values for r_0 are of interest where the curves reach the current maximum limit. From this figure it is also clear that the effort will increase exponentially since we are bound to a single thread for individual solving routines. Hence parallel computation of this problem would not help in this case especially considering that server processing units typically have lower single threaded

[7] Thread refers to a sequence of instructions given to a processing unit.

performance than consumer chips.
Explicit parallelisation is achieved by distributing different values of n to different threads. More efficient distribution of those calculations can make a difference but effects discussed above and below have more impact. Furthermore in order to fully understand how to improve for this distribution it is partly necessary to calculate the results which is then even less of an issue afterwards.
Another optimisation evolved around not computing unnecessary cases. Consider again figure 6. It is clear (however not proven until now) that for each combination A, p_0 at some value $n_0(A, p_0)$ values for r_0 will reach the numerical upper limit of the routine. For other solving routines with $n \geq n_0$ the same will happen which makes it unnecessary to even begin to compute them since they will not be shown in the graph anyways. This behaviour has been verified for a number of numerical combinations of parameters before beeing utilised in the final version. For the solving routine this means explicitly that once there have been 2 previous solving routines that failed in obtaining a value lower than r_0, the whole routine will not consider solving for any combinations of these particular parameters A, p_0 anymore.
Another obvious optimisation was to use a database to store results. In this case MongoDB [DH21] was chosen for its good integration with the python language. This pool of results allows one to compare the current solving routine with already calculated results. Extra calculations can be permitted after a database query in the following cases:

- If the current solving routine does have higher precision (in form of lower constant stepsize).
- If the previous solving routine reached the limit for r_0 and the current one would go further.
- If there exist multiple results for a combination of parameters A, p_0, n [8].

With these optimisations less results in total need to be calculated. One still present disadvantage is however that allocation of parameters for solving routines is done beforehand and can not be changed in mid process. This means if a thread started by the program finished and another is still running with multiple solving routines left, these cannot be given to another thread. This is a possibility for future tweaks.
So far the previous discussion evolved around a fixed stepsize. Since in this case the 4th order Runge Kutta solving method was implemented by hand, it is possible to use variable stepsizes for solving. From figure 4 we can see that the largest errors occur in the first step of integration. This means in the beginning a small stepsize is desireable to retain accuracy while later it can be increased. These settings were experimented with but since the author had already achieved numerous results with a constant stepsize were not committed to the final version. It is however believed to yield a significant advantage if one would want to calculate higher values of r_0.

[8] Then every result present is deleted and one new result will be calculated.

References

[AS84] Milton Abramowitz and Irene A. Stegun, eds. *Pocketbook of Mathematical Functions. Abridged Edition of "Handbook of Mathematical Functions" by Milton Abramowitz and Irene A. Stegun. Material Selected by Michael Danos and Johann Rafelski*. English. 1984. ISBN: 978-3-87144-818-8. URL: https://www.zbmath.org/?q=an%3A0643.33002 (visited on 03/10/2021).

[Ban22] Stefan Banach. "Sur les opérations dans les ensembles abstraits et leur application aux équations intégrales". pl. In: *Fundamenta Mathematicae* 3 (1922), pp. 133–181. ISSN: 0016-2736, 1730-6329. DOI: 10.4064/fm-3-1-133-181.

[CD00] Yvonne Choquet-Bruhat and Cécile Dewitt-Morette. *Analysis, Manifolds and Physics, Part II*. en. Elsevier, 2000. ISBN: 978-0-444-50473-9.

[Cha58] Subrahmanyan Chandrasekhar. *Chandrasekhar-An Introduction To The Study Of Stellar Structure*. English. Astrophysical Monographs. Yerkes Observatory: Dover Publications, 1958. ISBN: 0-486-60413-6. URL: https://ia800602.us.archive.org/26/items/AnIntroductionToTheStudyOfStellarStructure/Chandrasekhar-AnIntroductionToTheStudyOfStellarStructure.pdf.

[Cho09] Yvonne Choquet-Bruhat. *General Relativity and the Einstein Equations*. en. Oxford Mathematical Monographs. Oxford ; New York: Oxford University Press, 2009. ISBN: 978-0-19-923072-3.

[Cho15] Yvonne Choquet-Bruhat. *Introduction to General Relativity, Black Holes, and Cosmology*. en. First edition. Vol. 52. Oxford: Oxford University Press, Aug. 2015. ISBN: 978-0-19-966645-4. URL: http://choicereviews.org/review/10.5860/CHOICE.191353 (visited on 06/18/2020).

[DH21] Mike Dirolf and Bernie Hackett. *Pymongo 3.11.3, Python Driver for MongoDB*. MongoDB, Inc. pypi.org/project/pymongo/, Feb. 2021. URL: https://pypi.org/project/pymongo/.

[Esc11] Helmut Eschrig. *Topology and Geometry for Physics*. en. Vol. 822. Lecture Notes in Physics. Berlin, Heidelberg: Springer Berlin Heidelberg, 2011. ISBN: 978-3-642-14699-2 978-3-642-14700-5. DOI: 10.1007/978-3-642-14700-5. URL: http://link.springer.com/10.1007/978-3-642-14700-5 (visited on 06/18/2020).

[Fli18] Torsten Fließbach. *Statistische Physik: Lehrbuch zur Theoretischen Physik IV*. de. Berlin, Heidelberg: Springer Berlin Heidelberg, 2018. ISBN: 978-3-662-58032-5 978-3-662-58033-2. DOI: 10.1007/978-3-662-58033-2. URL: http://link.springer.com/10.1007/978-3-662-58033-2 (visited on 03/10/2021).

[Fli20] Torsten Fließbach. *Mechanik: Lehrbuch zur Theoretischen Physik I*. de. Berlin, Heidelberg: Springer Berlin Heidelberg, 2020. ISBN: 978-3-662-61602-4 978-3-662-61603-1. DOI: 10.1007/978-3-662-61603-1. URL: http://link.springer.com/10.1007/978-3-662-61603-1 (visited on 03/10/2021).

[HSW10] Musa H., Ibrahim Saidu, and Marianus Waziri. "A Simplified Derivation and Analysis of Fourth Order Runge Kutta Method". In: *International Journal of Computer Applications* 9 (Nov. 2010). DOI: 10.5120/1402-1891.

[Kut01] Wilhelm Kutta. "Beitrag zur näherungsweisen Integration totaler Differentialgleichungen." German. In: Zeitschrift für Mathematik und Physik 46 (1901), p. 678. URL: https://books.google.de/books?id=QL0KAAAAIAAJ.

[Noe08] Peter D. Noerdlinger. "Solar Mass Loss, the Astronomical Unit, and the Scale of the Solar System". In: *arXiv:0801.3807 [astro-ph]* (Jan. 2008). arXiv: 0801.3807 [astro-ph]. URL: http://arxiv.org/abs/0801.3807 (visited on 04/12/2021).

[Ple21] Jonas Pleyer. *Github Repository by Jonas Pleyer*. en. 2021. URL: https://github.com/jonaspleyer (visited on 04/18/2021).

[QS07] Pavol Quittner and Philippe Souplet. *Superlinear Parabolic Problems: Blow-up, Global Existence and Steady States*. en. Birkhäuser Advanced Texts : Basler Lehrbücher. Basel: Birkhäuser, 2007. ISBN: 978-3-7643-8442-5.

[Run95] C. Runge. "Ueber die numerische Auflösung von Differentialgleichungen". de. In: *Mathematische Annalen* 46.2 (June 1895), pp. 167–178. ISSN: 1432-1807. DOI: 10.1007/BF01446807. URL: https://doi.org/10.1007/BF01446807 (visited on 04/14/2021).

[Spiec] Michael Spivak. *Physics for Mathematicians, Mechanics I*. Englisch. first. Houston, Tex.: Publish or Perish, 2010, dec. ISBN: 978-0-914098-32-4.

[Vin17] Jorick S. Vink. "Mass Loss and Stellar Superwinds". In: *Philosophical Transactions of the Royal Society A: Mathematical, Physical and Engineering Sciences* 375.2105 (Oct. 2017), p. 20160269. DOI: 10.1098/rsta.2016.0269. URL: https://royalsocietypublishing.org/doi/10.1098/rsta.2016.0269 (visited on 04/12/2021).

[Wal84] Robert M. Wald. *General Relativity*. Chicago: University of Chicago Press, 1984. ISBN: 978-0-226-87032-8.

[Wei20] Eric W. Weisstein. *Lane-Emden Differential Equation*. en. Text. Dec. 2020. URL: https://mathworld.wolfram.com/Lane-EmdenDifferentialEquation.html (visited on 12/28/2020).

Erklärung

Hiermit versichere ich, dass ich die eingereichte Masterarbeit selbständig verfasst habe. Ich habe keine anderen als die angegebenen Quellen und Hilfsmittel benutzt und alle wörtlich oder sinngemäß aus anderen Werken übernommenen Inhalte als solche kenntlich gemacht. Weiter versichere ich, dass die eingereichte Masterarbeit weder vollständig noch in wesentlichen Teilen Gegenstand eines anderen Prüfungsverfahrens war oder ist.

Ort und Datum

Unterschrift